# Molecular dynamics of a liquid drop spreading in a corner formed by two planar substrates

Chi-Chuan Hwang*
*Department of Engineering Science, Natiional Cheng Kung University, Tainan, Taiwan 701, Republic of China*

Jeng-Rong Ho
*Department of Mechanical Engineering, National Chung Cheng University, Chia Yi, Taiwan 621, Republic of China*

Shio-Chao Lee
*Department of Electronic Engineering, Minghsin Institute of Technology, Hsin Chu, Taiwan 304, Republic of China*
(Received 8 September 1998; revised manuscript received 19 April 1999)

Molecular-dynamics simulations were used to investigate the spreading of nonvolatile liquid drops in a solid corner formed by two planar substrates. To understand the effect of the corner on the spreading, liquid drops in a corner with angles of 45°, 90°, and 135° as well as on a flat substrate were examined. Both the solid substrate and the liquid drop were modeled using the Lennard-Jones interaction potential in the present study. Simulation results show that the mass center of the liquid molecules migrated towards the corner as time evolved and the spreading rate increased as the corner angle decreased. It is found that the variation of the mean spreading area with time can be described by a general relation of $A(t) \sim t$, which is in agreement with results obtained by other investigators. The distribution of liquid atoms per unit normalized corner degree shows a similar trend for different corner angles. [S1063-651X(99)02311-9]

PACS number(s): 68.10.Gw, 68.45.Gd, 02.70.Ns, 61.20.Ja

## I. INTRODUCTION

The spreading of liquids over solid surfaces has been considered an important problem with practical significance in such diverse fields as painting, adhesion, lubrication, and tertiary oil recovery. Understanding the spreading dynamics can also aid the development of submicron manufacturing techniques, including surface coating, etching, doping, and thin-film growth. Various theoretical models have been proposed, based on continuum mechanics approaches, to describe the static and dynamic process of wetting [1–12]. In his review article on wetting, de Gennes [2] discussed in detail various wetting phenomena with special emphasis on the features of ''dry spreading.'' He indicated that the final state of a spreading drop is not necessarily a monomolecular thick film. Depending on the way the driving forces are categorized, the spreading of liquids on solids is usually divided into three types: primary, secondary, and bulk. The thickness of the liquid film ranges from several particles to microns. Teletzke *et al.* proposed a theory of wetting which accounts for multiple driving forces, including the capillary pressure gradient, gravitational potential gradient, surface tension gradient, disjoining pressure gradient, and surface diffusion [3]. During the process of complete wetting, a precursor liquid film of submicrometer thickness spreads ahead of the macroscopically liquid edge [2]. The growth rates, both in range and in thickness, of this precursor film have been widely discussed in experimental and theoretical works [5,7–11,13]. In some cases the growth rate of the precursor film is proportional to $\sqrt{t}$.

Molecular-dynamics simulation has also been employed to study the phenomenon of liquids spreading on solids [14–26]. This method can provide further insight, especially in those ranges for which the continuum fluid mechanics model is not suitable, as in the case of an ultrathin liquid film whose thickness is on the order of molecular length. Yang and coworkers [14,15] carried out molecular-dynamics studies on drop spreading on a solid surface. By increasing the strength of the attraction potential between the solid and liquid, the transition of regimes from partial wetting to terraced wetting could be observed. The spreading rate of terraced wetting was proposed to be $R^2(t) \sim \log_{10}(t)$. From the results of molecular-dynamics simulation, Nieminen *et al.* [17] found that molecular precursor film spreads at different rates: initially with constant speed, followed by a transition to diffusive spreading, and slowing down later on. Hanntaja *et al.* [21] studied the microscopic structure of spreading precursor film using the molecular-dynamics technique. In their simulation, the liquid drop was composed of dimmers with chainlike particles. From their molecular-dynamics study, Bekink *et al.* [22] concluded that the radii of the terraced layers vary with $\sqrt{t}$, regardless of system size, lattice geometry, and thermostating. They argued that different growth rates in previous studies were due to the porosity of the lattice. De Coninck *et al.* [28] studied a two-dimensional Ising drop in a corner, and concluded that varying the corner angle affects the final wetting status but does not affect the spreading dynamics.

The above literature review shows that most molecular-dynamics studies on spreading phenomena have investigated liquid drops on flat solid substrates. To the authors' knowledge, no works on liquid drops spreading in corners have been presented. It would be very interesting to know how corners affect the spreading dynamics of liquid drops. In this

*Author to whom correspondence should be directed. FAX: 886-6-2766549. Electronic address: chchwang@mail.ncku.edu.tw

 

work, we will present the spreading dynamics of a liquid drop in a corner with angles of 45°, 90°, and 135°. The dependence of the growth rate of the mean-spreading region on the corner angles will be demonstrated systematically, and the effect of the solid-liquid attraction strength on the spreading dynamics will also be discussed.

## II. PHYSICAL MODEL AND SIMULATION METHOD

To simulate the spreading of a drop in a corner, we used a liquid drop and two planar solid substrates. The liquid drop was composed of 1372 molecules, which were initially assigned to an approximately spherical region of the face-centered-cubic lattice. The two solid substrates were formed from the simple cubic lattice. We calculated three geometric models, namely, the 45°, 90°, and 135° corners. For the 45° and the 135° corners, the height (the $z$ direction) of the first substrate, the horizontal one, was two atomic layers. Each layer consisted of 1200 atoms, which were arranged in a rectangular region 40 atomic layers in length (the $x$ direction) and 30 atomic layers in depth (the $y$ direction). For the 90° corner, each layer consisted of 1600 solid molecules, which were placed in a square region which was 40 atomic layers in both length and depth. The second substrate was modeled as follows. (i) For the 90° corner, there were two atomic layers in the $x$ direction. The width of $y$ and $z$ directions was 40 atomic layers; thus, the total number of atoms in this substrate was 3200. (ii) For the 45° corner, there were 30 atomic layers in the $y$ direction. Each layer formed an equilateral and right-angled triangle in the $x$-$z$ plane with dimensions of 21 atoms in the lateral sides. The total number of atoms in this substrate was 6930. (iii) For the 135° corner, the height in the $y$ direction was 30 atomic layers. Each layer formed an equilateral and right-angled triangle in the $x$-$z$ plane, but the atomic number in the lateral sides was 15. Thus, the total number for this substrate was 3600. The panels on the left side of Fig. 1 show the initial configuration of the three calculated geometric models, consisting of the liquid drop and the planar substrates.

The considered molecular system is described by Lennard-Jones interaction potentials of the form

$$u(r_{ij}) = 4\varepsilon\left[c_{ij}\left(\frac{\sigma}{r_{ij}}\right)^{12} - d_{ij}\left(\frac{\sigma}{r_{ij}}\right)^{6}\right], \tag{1}$$

where the subscript $ij$ represents the connection between pair particles of type $i$ and $j$, $r$ is the distance between particles $i$ and $j$, and the parameters $\varepsilon$ and $\sigma$ provide the scales of energy and distance, respectively. The coefficients of $c_{ij}$ and $d_{ij}$ are the material parameters corresponding to the repulsive and attractive intermolecular forces between two particles, respectively. In what follows, the symbols $d_{\mathrm{sl}}$ and $d_{\mathrm{ll}}$ will stand for the attractive parameters at the solid-liquid and the liquid-liquid interfaces, respectively. A parameter $\alpha$, defined as the ratio of $d_{\mathrm{sl}}$ to $d_{\mathrm{ll}}$, is used to represent the strength of the solid-liquid interaction. By varying this parameter, we can adjust the strength of attraction between solid and liquid atoms. For computational convenience, the energy scale $\varepsilon$, length scale $\sigma$, and the atomic mass scale $m$ are used to nondimensionalize all subsequent expressions. The resulting time-step unit is $\tau = t/\sigma\sqrt{m/\varepsilon}$. The dimensionless units for temperature, velocity, and atomic number density are, thus, defined as $T^* = kT/\varepsilon$, $v^* = v\sqrt{m/\varepsilon}$, and $\rho^* = N\sigma^3/V$, respectively. According to these definitions the diameter of the liquid drop was set to be 11.97, and the densities for the liquid drop and for the solid substrates were 0.8 and 1.0, respectively.

The initial positions of the mass center of the liquid drop were at (14.5, 9, 3.5), (3.5, 14, 3.5), and (14,9,5) for the 45°, 90°, and 135° corners, respectively. The atomic spacing was set to match the designed density, and a random kinetic energy drawn from a Boltzmann distribution, subject to a fixed temperature of 0.7, was then assigned to each atom. It was assumed that the mass of a solid atom was $10^{10}$ times larger than the mass of a liquid atom. This assumption made solid atoms motionless during our computations [27]. The initially instantaneous potential was specified after the position of atoms were given, and Newton's law of motion was numerically integrated using a fifth-order Gear's predictor-corrector algorithm with a time step of $0.005\tau$. To get rid of the boundary effects, periodic boundary condition was applied to all the boundaries of the substrates except the two corner surfaces facing the liquid drop. The simulated molecular system was further assumed to be an isolated system at a fixed temperature of 0.7. For the purpose of keeping the system at constant temperature, the total kinetic energy in the system was monitored and corrected at every time step during the computation. The strength of the solid-liquid interaction, $\alpha$, was set at 1.2 while the potentials of fluid-fluid interactions and fluid-solid interactions were cut off at $2.5\sigma$.

## III. RESULTS AND DISCUSSIONS

Initially, the molecules of the liquid drop were at thermal equilibrium and fluctuated because of their thermal motions. As our simulations started, those molecules that were located closer to the substrate surfaces experienced attractive forces from the substrate and moved towards the substrate surfaces. Spreading commenced. Once the liquid molecules were in contact with the substrates, they were absorbed on the substrate surfaces due to the stronger solid-liquid attractive force. The phenomenon of spreading became more clear as the number of absorbed atoms increased. Figure 2 shows snapshots of the side profile of the spreading drop at different times for the 45° corner. The solid-liquid interaction strength was fixed at $\alpha = 1.2$. Because the liquid drop was initially placed relatively closer to the horizontal substrate than to the inclined one, the liquid molecules interacted more obviously with the horizontal substrate during the early stage of spreading. When some liquid molecules reached the surface of the inclined substrate, at around $\tau = 75$, the effect of the second substrate became substantial. The spreading behavior indicated that the liquid drop interacted both simultaneously and independently with two flat planar substrates. As time went by, the liquid drop was attracted towards the corner, and the outer profile changed from convex to concave. Liquid molecules condensed on the substrate surface forming the ''condensed layers.'' As the spreading continued, from $\tau = 200$ to 300, molecules clustered in the corner region stretched out through sliding on the condensed layers, and layer spreading occurred at these times.

Qualitatively similar spreading processes were observed

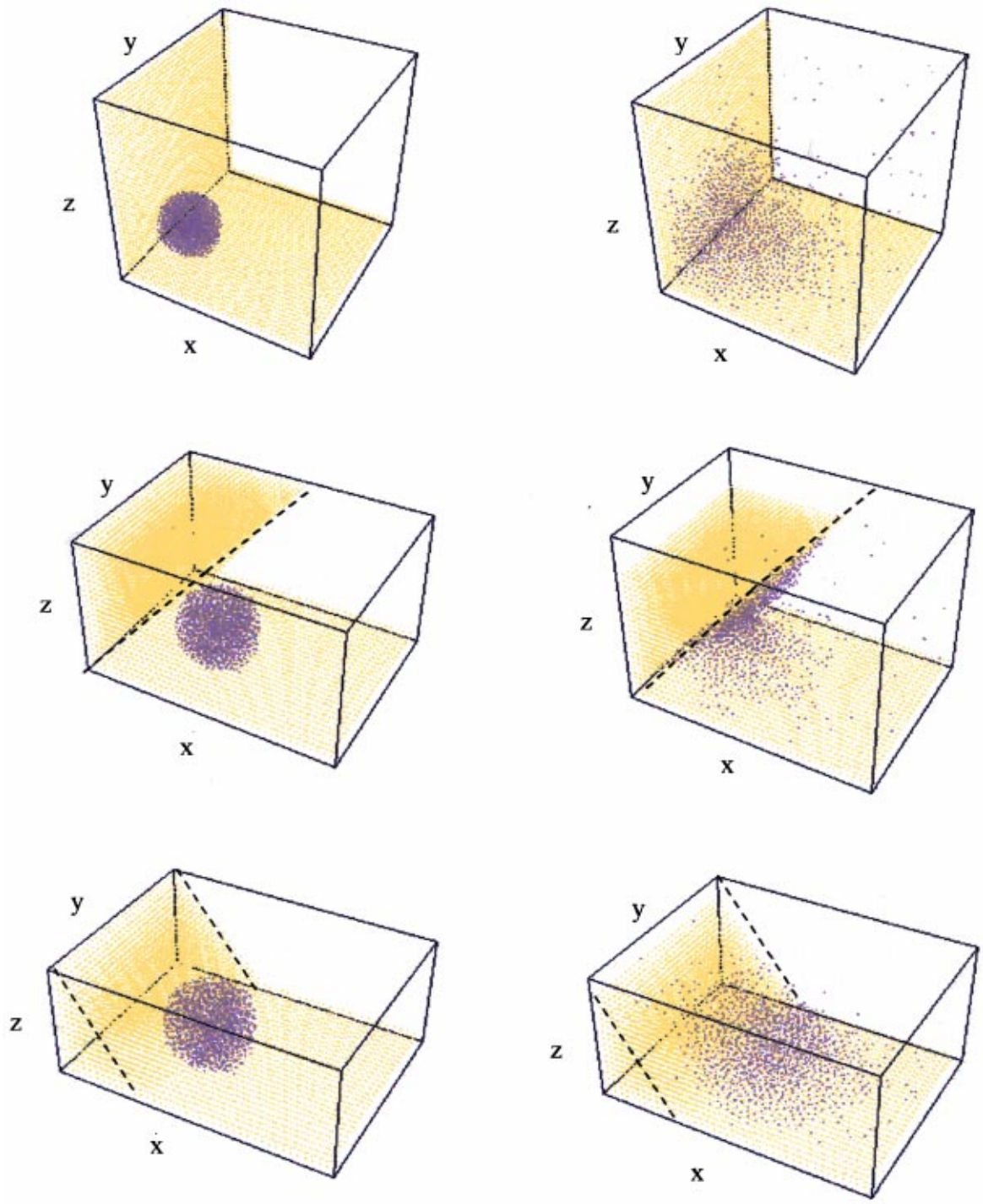


FIG. 1. (Color) Physical configurations showing the initial and final states of the liquid drop spreading in corners, from top to bottom, with angles of 45°, 90°, and 135°, respectively. The initial states before spreading are shown on the left side and the spreading states at $\tau = 300$ are shown on the right side.

as the corner angle increased to 90° and 135°. It was observed that the outer profile of the liquid drop was concave in shape with a contact angle of about 10° when $\alpha = 1.2$. To check the effect of the drop size on the spreading, we increased the number of molecules in the liquid drop to 2048 and 4000. We found that the spreading processes were qualitatively similar, but that the layer spreading was more observable for larger drop sizes.

The spreading rate of the precursor film in a corner was another interesting issue worth investigating. The mean-spreading area, describing the region covered by the condensed layer, was used to quantitatively capture the spreading rate. In Fig. 3, the time-varying, mean-spreading area for different corner angles is presented. Here the solid-liquid interaction strength is 1.2. In this figure, the slopes of lines, $S_1$ to $S_4$ represent the spreading rates for different corner angles, from 45° to 180°. It is seen that the smaller the corner angle is, the higher the spreading rate becomes. The reason is that the averaged distances between the liquid molecules and the substrate surfaces are relatively shorter for the smaller

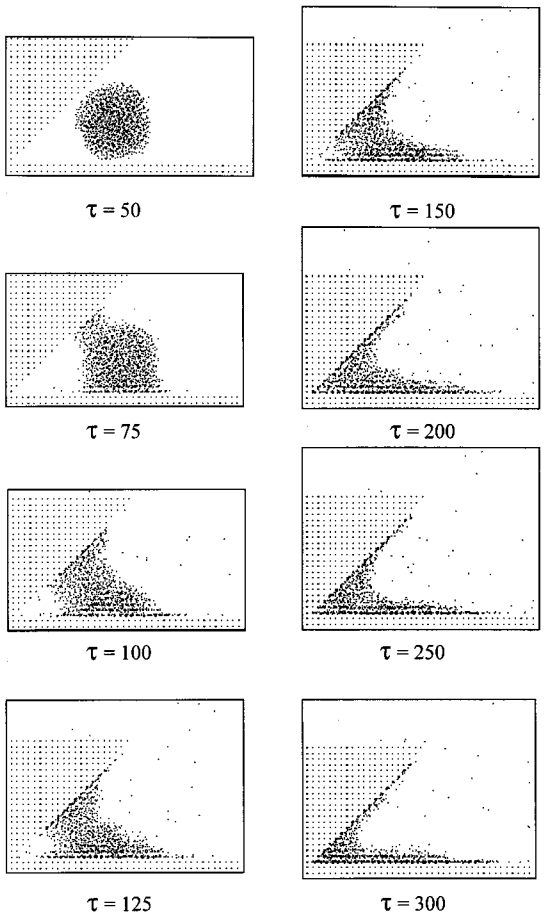


FIG. 2. Snapshots of the side profile of a liquid drop spreading a 45° corner at eight different times. The number of liquid atoms was 1372 and the number of solid atoms was 9330. The solid-liquid interaction strength, $\alpha$, was set at 1.2.

corner angle than for the larger corner angle. A generalized expression for the mean-spreading area versus time is

$$A(\tau)=S(\tau-\tau_0)^n, \tag{2}$$

where $\tau_0$ is the chosen reference time. If fitted to the computed results, the power $n$ is close to unit. This result is similar to the relations obtained in recent theoretical and experimental works [5,22], where the mean-spreading radii of layers varying with time is expressed as $R^2(\tau)\sim\tau$.

The distribution of the liquid atoms in the corner at $\tau=300$ is shown in Fig. 4. The abscissa is the dimensionless angle $\theta^*$, which is normalized based on the number of degrees in the corner angle and is measured anticlockwise from the horizontal substrate surface. The area under the distributive curve represents the number of liquid atoms within the corner. It is noted that the area decreases as the corner angle increases. This is due to the relatively higher evaporation rate for cases with larger corner angles. These curves show a common and similar distributive trend in that the number of atoms goes from a peak to a valley and then back to a peak as $\theta^*$ varies from 0 through 0.5 to 1.0. It is observed that the

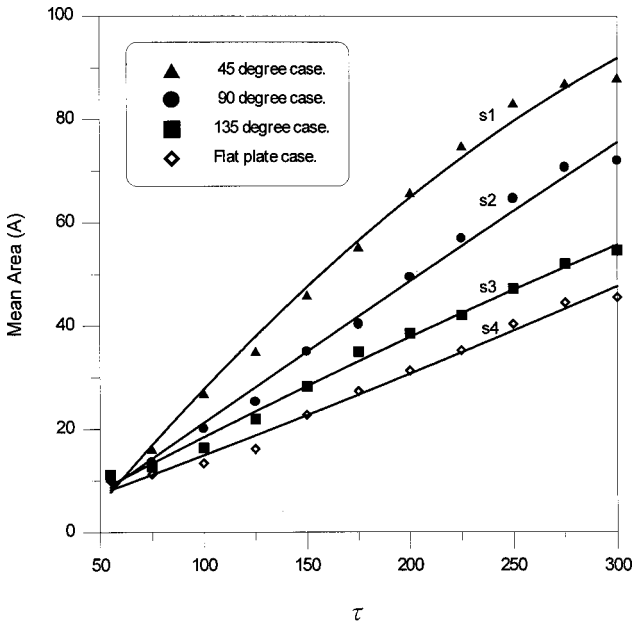


FIG. 3. Time dependence of the mean spreading area with different corner angles. The solid-liquid interaction strength was set at 1.2.

liquid atoms mainly accumulate close to the substrate surfaces and distribute symmetrically with respect to the corner center, $\theta^*=0.5$.

The velocity of a liquid atom on a solid surface is governed by the resulting force, formed from interactions of many atoms, acting on it. Figure 5 shows the time variance of the mean-spreading velocity of a liquid drop for different corner angles. The curves in this figure indicate that, during the early stage of spreading, the mean-spreading velocity increases rapidly from the atom's initial mean thermal velocity to a maximum; after this peak, it decreases faster at first than

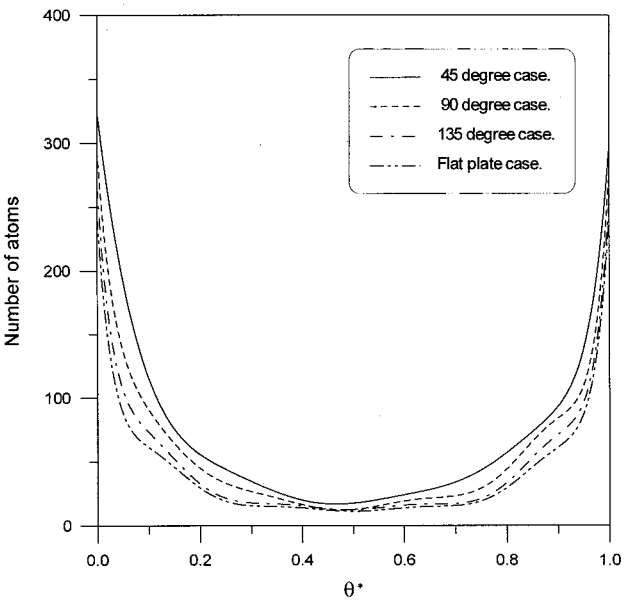


FIG. 4. Distribution of the liquid atoms in the corner. The dimensionless angle $\theta^*$ is normalized based on the number of degrees in the corner angle. The solid-liquid interaction strength was set at 1.2.

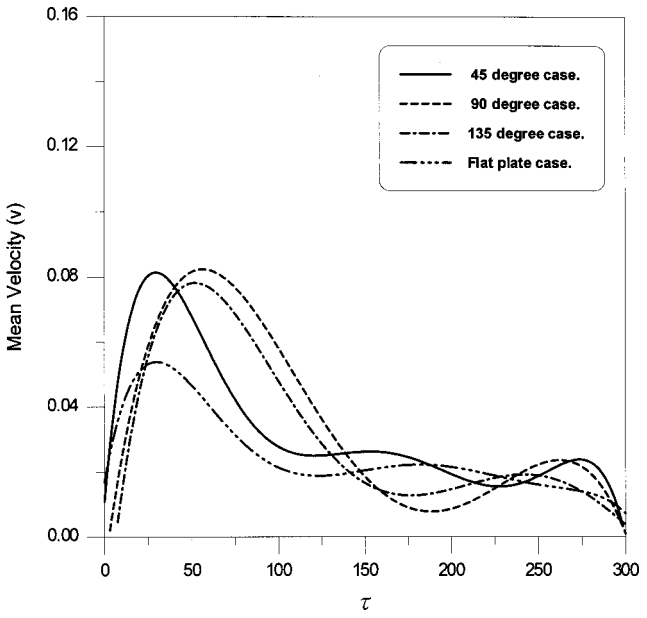


FIG. 5. Time variance of the mean-spreading velocity of a liquid drop spreading on substrate surfaces with different corner angles. The solid-liquid interaction strength was set at 1.2.

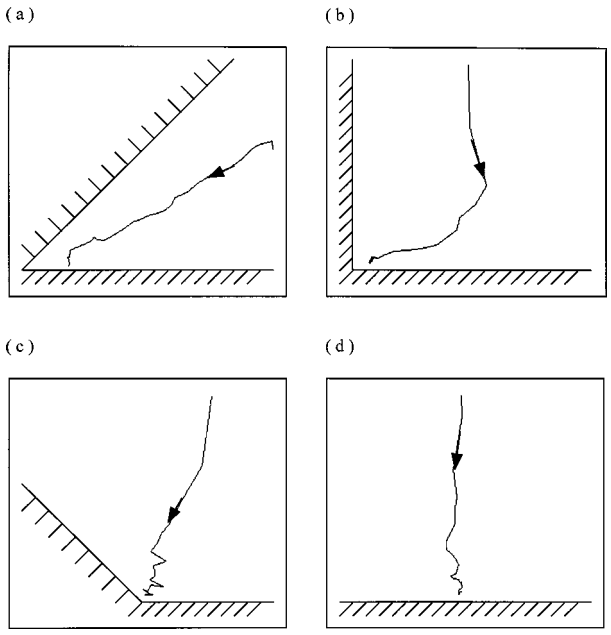


FIG. 6. Loci of the mass center of the liquid drop spreading in a corner with different corner angles. The solid-liquid interaction strength was set at 1.2.

slower versus time. Initially, the strong attraction between the bare substrate surface and the liquid molecules contributes to the rapid increase of the mean-spreading velocity. As more and more liquid atoms condense on the surfaces, the repulsive forces among the liquid atoms gradually increase. The maximum value of the mean velocity indicates an instantaneous balance between the attractive and repulsive forces. After the peak, the repulsive force continues to increase due to the motion inertia of liquid atoms. The decrease in the mean velocity is retarded when a new net force balance is reached at a later time. It is also noted that the appearance of the peak mean velocity is delayed as the corner angle increases. This indicates that the effect of the corner on drop spreading occurs relatively earlier for smaller corner angles than for larger corner angles.

In Fig. 6, we present the locus of the mass center of the liquid drop spreading in a corner with different angles. Macroscopically, this locus represents the motion of a liquid drop. From Figs. 6(a)–6(c), it is seen that the liquid drop moves from its initial position to an equilibrium position, the center of the center. In the 90° corner case, shown in Fig. 6(b), we put more liquid atoms with initial positions closer to the horizontal substrate than to the vertical substrate. The liquid drop first moves towards the horizontal substrate due to the stronger net attractive force from that substrate. As the wetting area increases in size, the influence from the vertical substrate is revealed. A clear turn is detected in the locus, where wall effects due to the vertical surface are no longer negligible. For spreading on a flat plate, the locus, shown in Fig. 6(d), looks like a vertical line. This is because the distribution of attractive forces from the substrate atoms is roughly symmetric with respect to the mass center of the liquid drop. The observed phenomenon, the migration of the mass center to the corner, is similar to the macroscopic results presented by Zia *et al.* [29].

## IV. CONCLUSIONS

A systematic study on the spreading of a liquid drop in a corner formed by two planar substrates has been carried out by means of molecular-dynamics simulation. Cases which have been studied include three cases with corner angles of 45°, 90°, and 135°, and one case on a flat plate. The liquid drop initially is spherical in shape and is located close to the two substrate surfaces. The substrate was modeled as being composed of almost motionless solid atoms. The time evolution of the spreading of the liquid drop has been presented. The influence of the solid-liquid attraction strength on the spreading has been considered. Three different sizes of the liquid drop, with molecule numbers of 1372, 2048, and 4000, have been employed in size-independence tests. The results can be summarized as follows.

(i) The vary of the mean-spreading area with time can be represented by the relation $A(t) \sim t$. This relation is applicable to liquid drop spreading on a flat plate as well as in a corner.

(ii) The smaller the corner angle, the stronger the wall effects, resulting in a higher spreading rate.

(iii) The distribution of liquid atoms per normalized unit degree shows similar trends for different corner angles.

## ACKNOWLEDGMENTS

The authors are grateful for the financial support provided by the National Center for High-performance Computing of the Republic of China (Grant No. NSC 87-WFD-05-C004-0018).

[1] E. B. Dussan, Annu. Rev. Fluid Mech. **11**, 371 (1979).
[2] P. G. De Gennes, Rev. Mod. Phys. **57**, 827 (1985).
[3] G. F. Teletzke, H. T. Davis, and L. E. Scriven, Chem. Eng. Commun. **55**, 41 (1987).
[4] P. Ball, Nature (London) **338**, 624 (1989).
[5] F. Heslot, A. M. Cazabat, and P. Levinson, Phys. Rev. Lett. **62**, 1286 (1989).
[6] L. Leger and P. Silberzan, J. Phys. **2**, SA421 (1990).
[7] J. Cook and D. E. Wolf, J. Phys. A **24**, L351 (1991).
[8] D. B. Abraham, J. Heinio, and K. Kaski, J. Phys. A **24**, L309 (1991).
[9] A. Chakrabarti, Phys. Rev. B **45**, 6286 (1992).
[10] M. Brenner and A. Bertozzi, Phys. Rev. Lett. **71**, 593 (1993).
[11] J. de Coninck, F. Dunlop, and F. Menu, Phys. Rev. E **47**, 1820 (1993).
[12] N. Fraysse, M. P. Valignat, A. M. Cazabat, F. Heslot, and P. Levinson, J. Colloid Interface Sci. **158**, 27 (1993).
[13] J. A. Mann, Jr., L. Romero, R. R. Rye, and F. G. Yost, Phys. Rev. E **52**, 3967 (1995).
[14] J. Koplik, J. R. Banavar, and J. F. Eillemsen, Phys. Fluids A **5**, 781 (1989).
[15] J. X. Yang, J. Koplik, and J. R. Banavar, Phys. Rev. Lett. **67**, 3539 (1991).
[16] J. X. Yang, J. Koplik, and J. R. Banavar, Phys. Rev. A **46**, 7738 (1992).
[17] J. A. Nieminen, D. B. Abraham, M. Karttunen, and K. Kaski, Phys. Rev. Lett. **69**, 124 (1992).
[18] S. M. Thompson and K. E. Gubbins, J. Chem. Phys. **81**, 530 (1984).
[19] D. J. Evans and W. G. Hovver, Annu. Rev. Fluid Mech. **18**, 243 (1986).
[20] I. Bitsanis, J. J. Magda, M. Tirrell, and H. T. Davis, J. Chem. Phys. **87**, 1733 (1987).
[21] M. Haataja, J. A. Nieminen, and T. Ala-Nissila, Phys. Rev. E **52**, R2165 (1995).
[22] S. Bekink, S. Karaborni, G. Verbist, and K. Esselink, Phys. Rev. Lett. **76**, 3766 (1996).
[23] J. Koplik and J. R. Banavar, Annu. Rev. Fluid Mech. **27**, 257 (1995).
[24] J. Koplik and J. R. Banavar, Phys. Fluids **7**, 3118 (1995).
[25] J. Koplik and J. R. Banavar, Phys. Rev. Lett. **78**, 2116 (1997).
[26] J. Koplik and J. R. Banavar, J. Rheol. **41**, 787 (1997).
[27] J. Koplik and J. R. Banavar, Phys. Fluids A **5**, 521 (1993).
[28] J. De Coninck, J. Fruttero, and A. Ziermann, Physica A **199**, 243 (1993).
[29] R. P. Zia, J. E. Arvon, and J. E. Taylor, J. Stat. Phys. **50**, 727 (1988).